Supporting information

Dual-Site Mediated Hydrogenation Catalysis on Pd/NiO: Selective Biomass Transformation and Maintaining Catalytic Activity at Low Pd Loading.

Sebastiano Campisi[†], Carine E. Chan-Thaw[†], Lidia E. Chinchilla[‡], Arunabhiram Chutia[#], Gianluigi A. Botton[‡], Khaled. M. H. Mohammed[§,¢], Nikolaos Dimitratos[¥], Peter P. Wells[§,◊,○*] and Alberto Villa[†*]

† Dipartimento di Chimica, Università degli Studi di Milano, via Golgi 19, 20133 Milano, Italy.

‡ McMaster University, Department of Materials Science and Engineering, Hamilton, Ontario, L8S 4M, Canada.

School of Chemistry, University of Lincoln, Lincoln, LN6 7TS.

§ School of Chemistry, University of Southampton, University Road, Southampton, SO17 1BJ, United Kingdom.

¢ Department of Chemistry, Faculty of Science, Sohag University, Sohag, P.O.Box 82524, Egypt.

¥ Dipartimento di Chimica Industriale "Toso Montanari", Alma Mater Studiorum, University of Bologna, Viale Risorgimento 4, 40136, Bologna, Italy.

◊ UK Catalysis Hub, Research Complex at Harwell, Rutherford Appleton Laboratory, Harwell Oxon, Didcot, OX11 0FA.

○ Diamond Light Source Ltd., Harwell Science and Innovation Campus, Chilton, Didcot OX11 0DE, United Kingdom.

Corresponding Author

* Email: p.p.wells@soton.ac.uk.
* Email: alberto.villa@unimi.it.

Figure S1. XRD patterns of NiO.

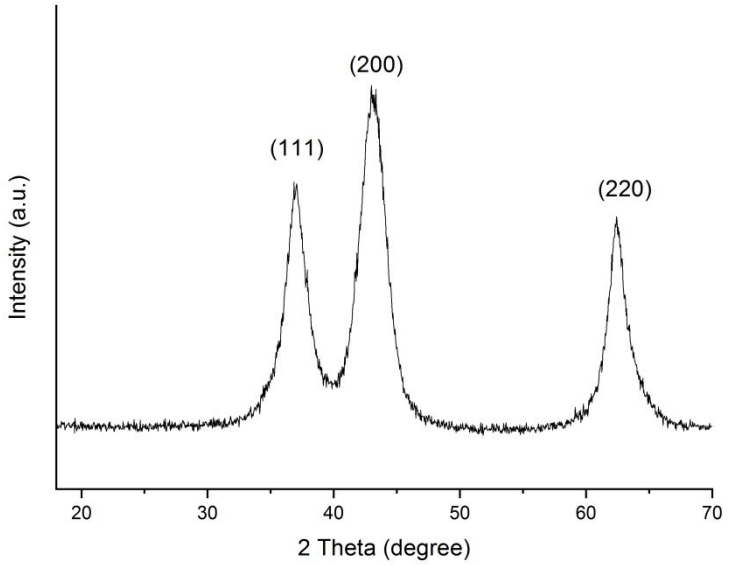

Figure S2. Pd 3d XPS data for (a) Pd/NiO, (b) Pd/TiO_2 and (c) Ni2p3/2 XPS data for NiO.

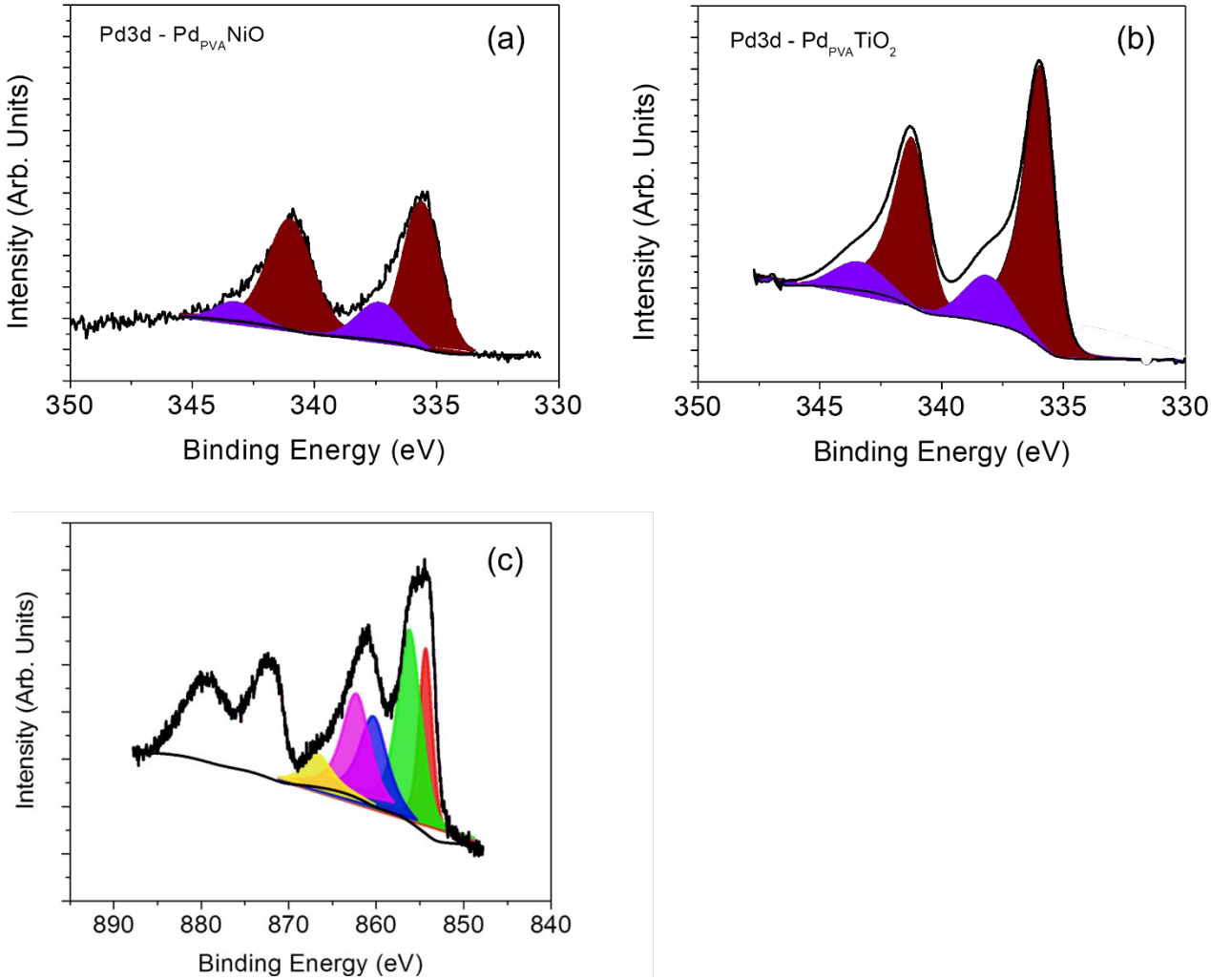

Figure S3. Reaction profile for 1 wt% Pd/TiO_2 and b) 1 wt% Pd/NiO.

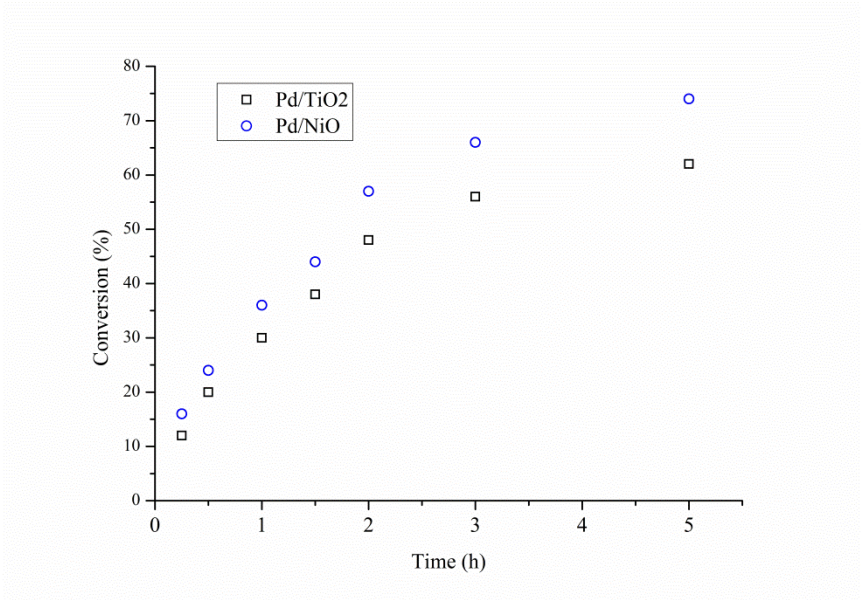

Figure S4. Selectivity vs conversion for a) 1 wt% Pd/TiO_2 and b) 1 wt% Pd/NiO.

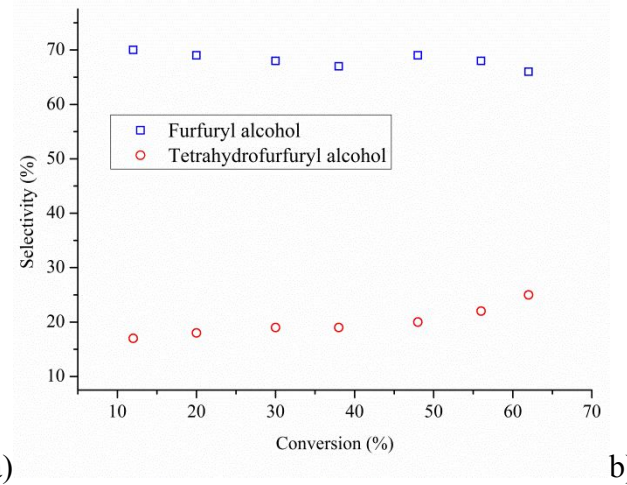

a)

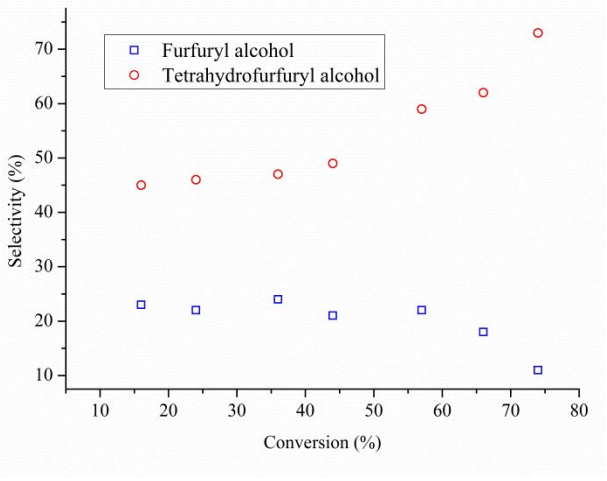

b)

Figure S5. Particle size distribution for a) 1 wt% Pd/TiO_2 and b) 1wt% Pd/NiO.

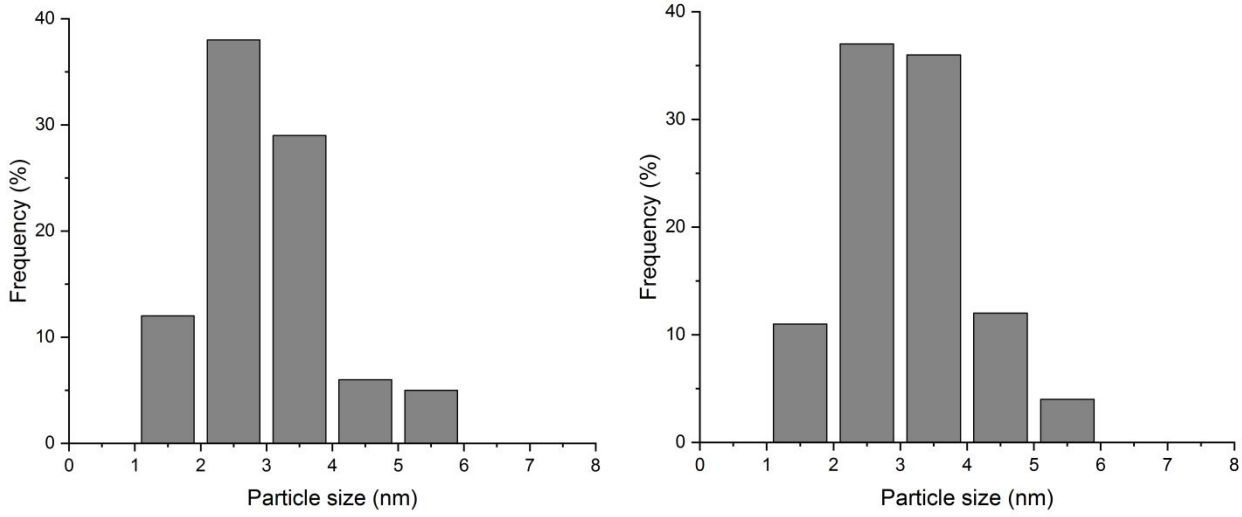

a) **b)**

Figure S6. High resolution STEM-HAADF images of 1 wt% Pd/NiO catalyst showing a crystalline particle (a) and sub nanometer species of Pd distributed across the support (b). Results of EELS-SI measurement, showing the HAADF image (c) and artificially colored overlay of Pd (green) and NiO (pink) maps (d). Bottom are independent components spectra and their corresponding distribution determined through machine learning methods implemented in Hyperspy.

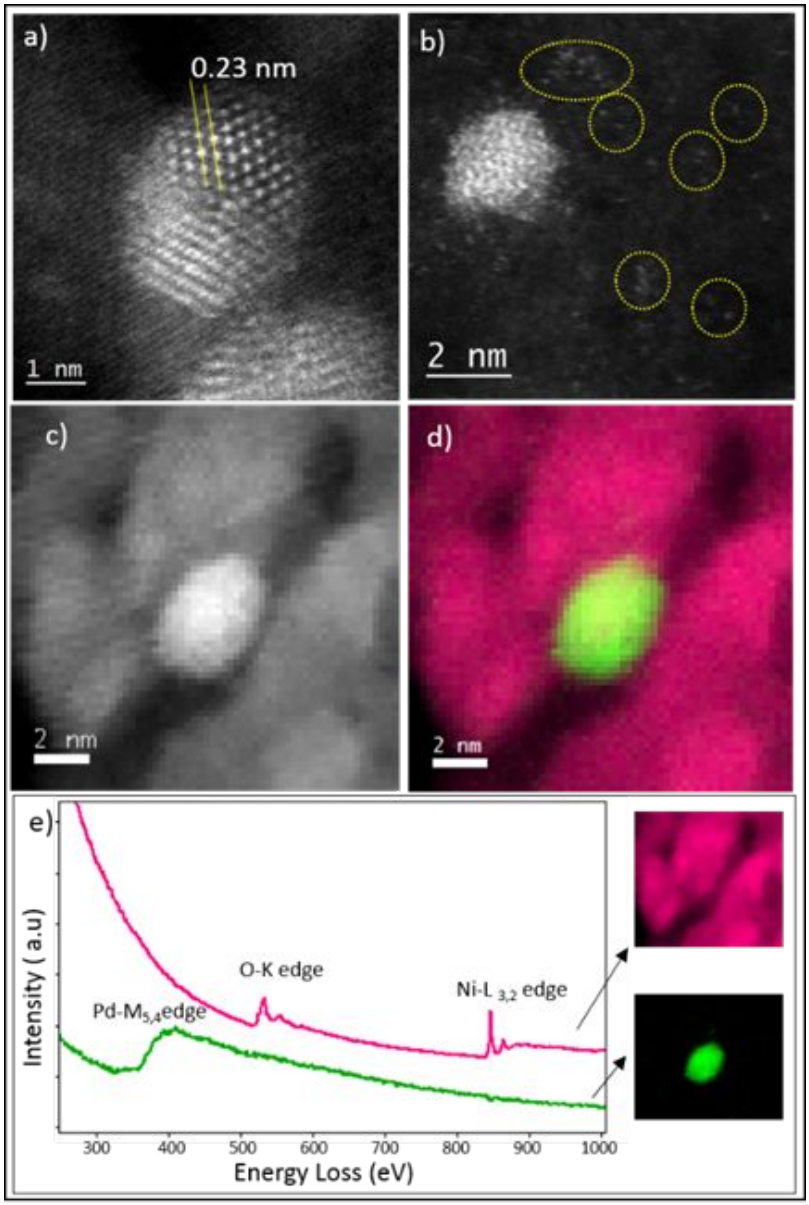

Figure S7. Optimized geometries of perpendicular configurations of furfural on (a) top of Pd atom (Pd_{top}), (b) bridge between to Pd-atoms (Pd_{bdg}), and (c) hollow site in-between three Pd-atoms (Pd_{hollow}). The optimized geometries of parallel configurations of furfural on Pd(111) (d) Conf.1, (e) Conf.2 and (f) Conf.3.

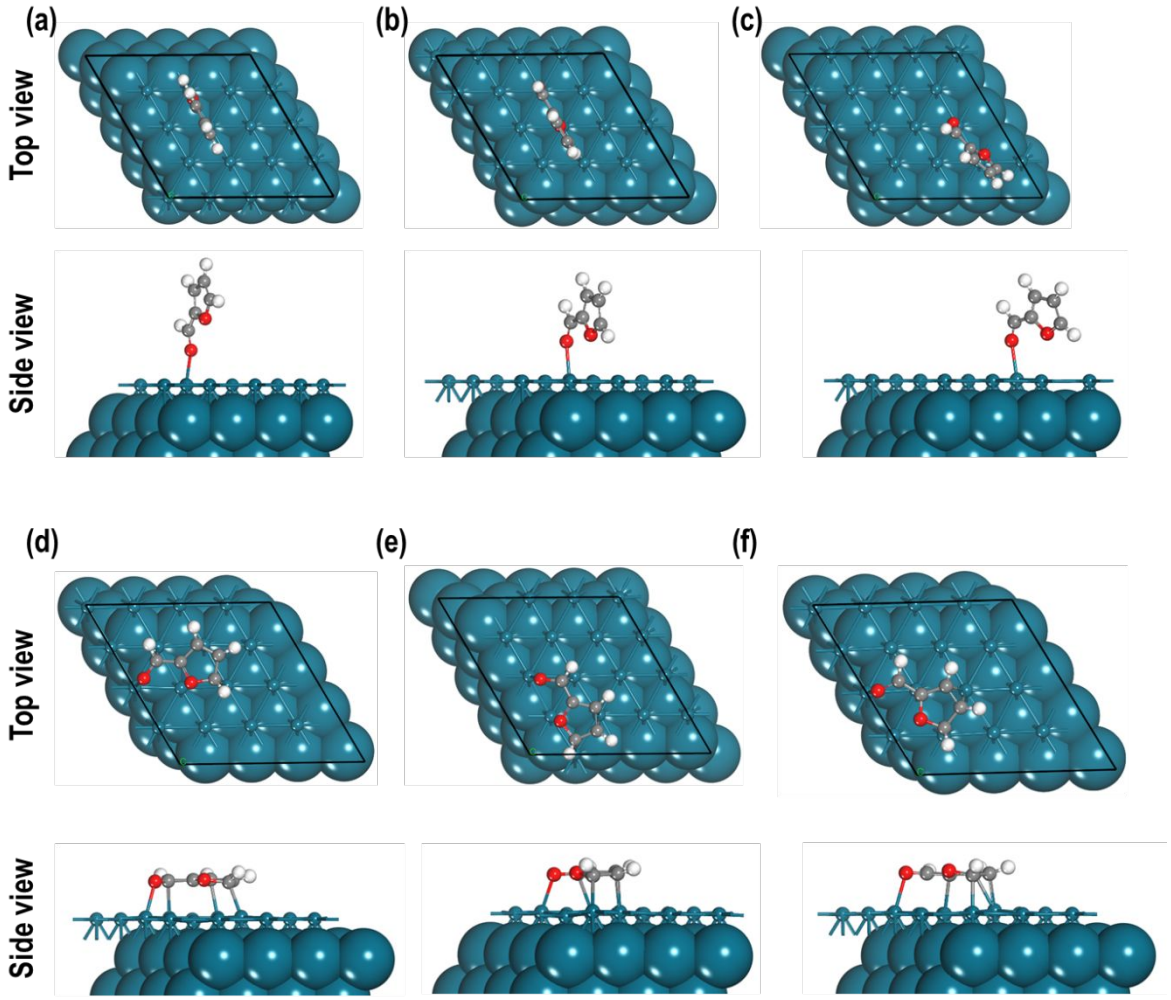

Figure S8. Optimized geometries of (a) NiO_conf1, (b) NiO_conf2, (c) NiO_conf3, (d) NiO_conf4, (e) NiO_conf5, (f) NiO_conf6, (g) NiO_conf7, (h) NiO_conf8, (i) NiO_conf9, (j) NiO_conf10, (k) NiO_conf11, (l) NiO_conf12, (m) NiO_conf13, (n) NiO_conf14, (o) NiO_conf15, (p) NiO_conf16, (q) NiO_conf17, (r) NiO_conf18, (s) NiO_conf19.

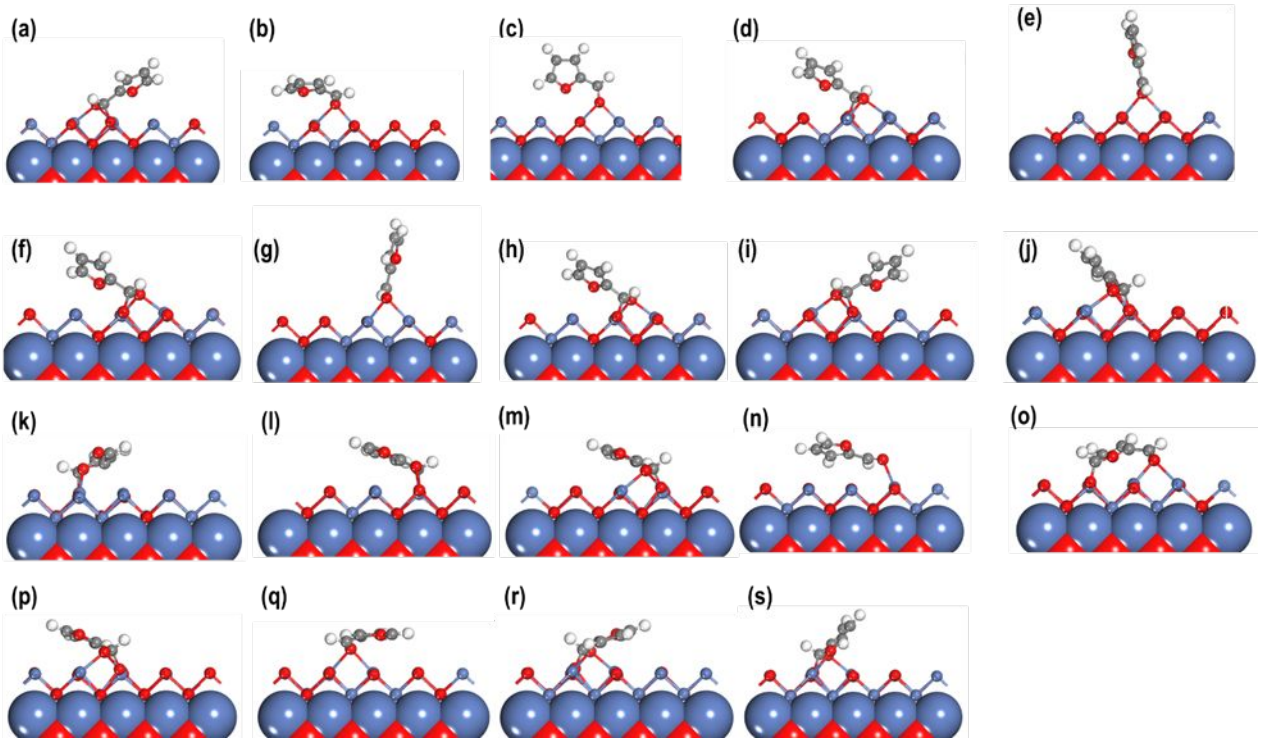

Figure S9. Optimized geometries of (a) TiO_2_conf1, (b) TiO_2_conf2, (c) TiO_2_conf3, (d) TiO_2_conf4, (e) TiO_2_conf5, (f) TiO_2_conf6, (g) TiO_2_conf7, (h) TiO_2_conf8, (i) TiO_2_conf9, and (j) TiO_2_conf10.

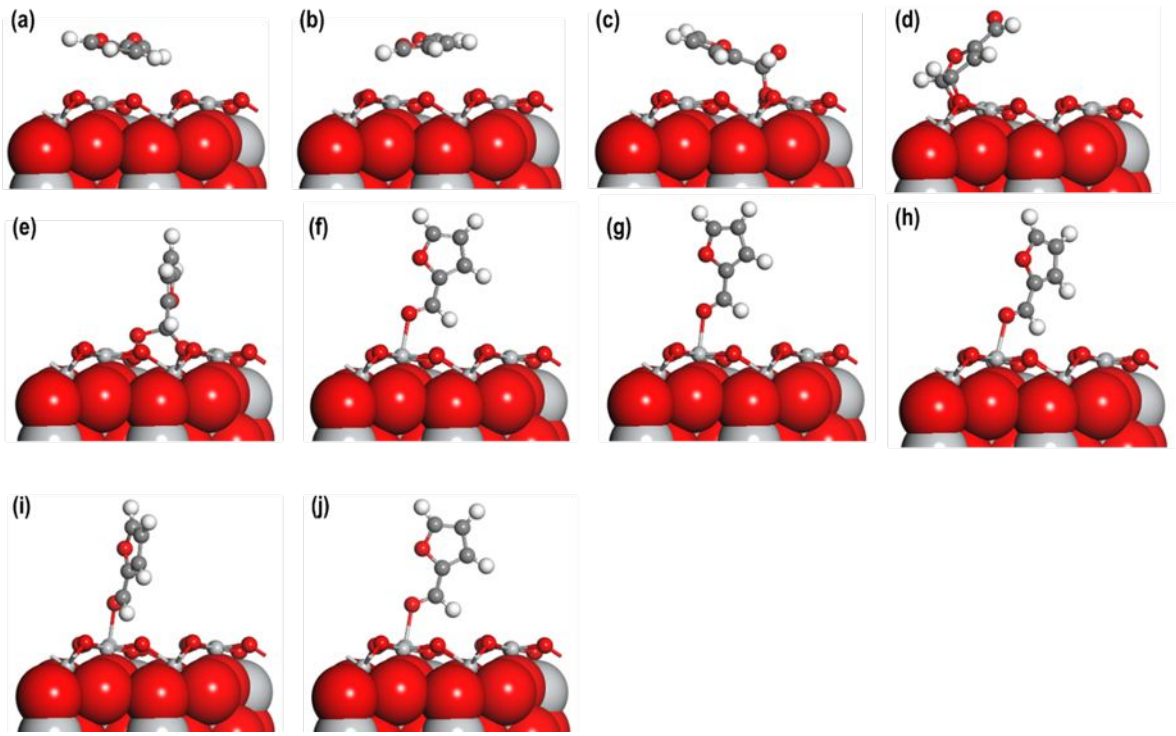

Figure S10. Optimised structures of (a) furfural parallel (E_{ad} = -1.946 eV), (b) furfural on top of Pd-atom (E_{ad} = -0.396 eV), (c) furfural in between two Pd-atoms (E_{ad} = -0.964 eV), (d) furfural in the HCP (E_{ad} = -1.017 eV) site of Pd_{16}-NiO(110) systems.

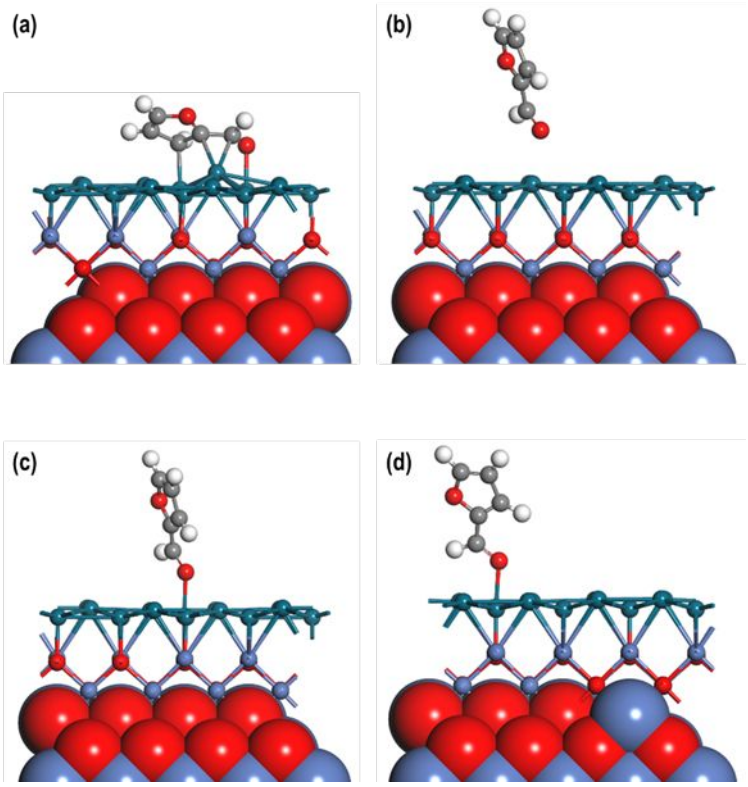

Figure S11. The energy barrier for the for the forward and reverse reaction of H_2 dissociation.

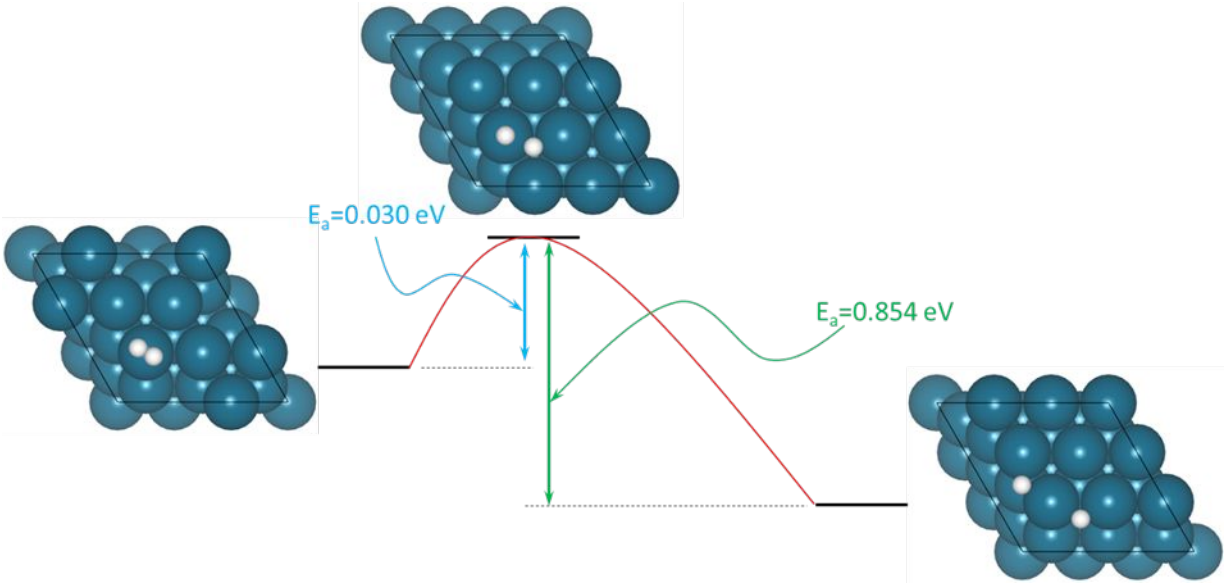

Figure S12. Particle size distribution for a) 0.1 wt% Pd/TiO_2 and b) 0.1 wt% Pd/NiO.

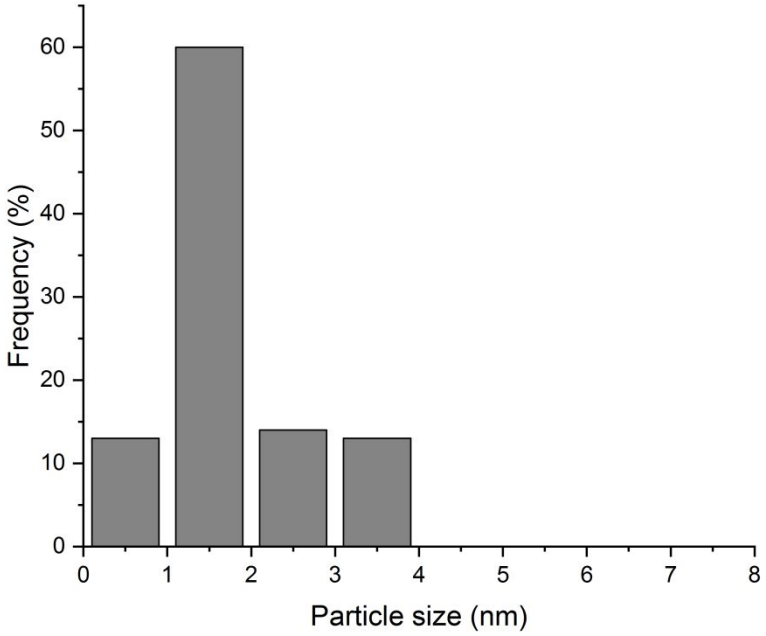

a)

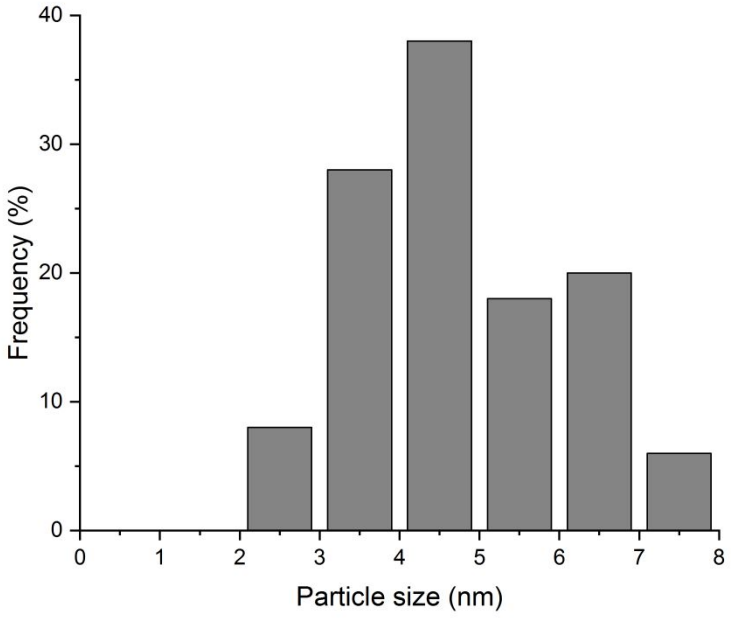

b)

Table S1. Furfural hydrogenation at 50 °C using 1 wt% Pd/NiO: influence of catalyst amount.

F/Metal ratio[a]	Activity[b] mol (metal mol)$^{-1}$ h^{-1}	Selectivity (%)[c]						
		Furfuryl alcohol	Tetrahydro Furfuryl Alcohol	2-methyl furan	2-methyl tetrahydro Furan	Furan	Ethers 1	Ethers 2
1/250	480	9	78	-	7	-	-	5
1/500	470	14	72	1	5	1	-	3
1/1000	485	21	65	-	3	-	3	2

[a] Reaction conditions: Furfural = 0.3 M, 50 °C, 5 bar H_2, solvent 2-propranol
[b] Mol of furfural converted per hour per mol of metal, calculated after 15 min reaction
[c] Selectivity at 60% conversion
[d] Selectivity at 10% conversion

Table S2. The calculated adsorption energies of 19 different models used to investigate the interaction of furfural on NiO(100) surface. The orientation of the initial and final geometry followed by the nature of interaction between furfural and NiO(100) has been also summarised.

System	Orientation		Bonded	Ead
	Initial	Final	through	
NiO_conf1	Perpendicular	Slanted	Aldehyde O & C	-2.218
NiO_conf2		Slanted	Aldehyde O	-1.579
NiO_conf3		Perpendicular	Aldehyde O	-1.280
NiO_conf4		Slanted	Aldehyde O & C	-2.319
NiO_conf5		Perpendicular	Aldehyde O	-1.151
NiO_conf6		Slanted	Aldehyde O & C	-2.345
NiO_conf7		Perpendicular	Aldehyde O	-1.152
NiO_conf8		Slanted	Aldehyde O & C	-2.290
NiO_conf9	Parallel	Slanted	Aldehyde O & C	-2.322
NiO_conf10		Slanted	Aldehyde O & C Furanic O	-2.572
NiO_conf11		Slanted	Furanic O & C	-1.075
NiO_conf12		Slanted	Aldehyde C	-2.291
NiO_conf13		Slanted	Aldehyde O & C	-2.405
NiO_conf14		Slanted	Aldehyde O	-1.149
NiO_conf15		Parallel distorted	Aldehyde O Furanic C	-2.013
NiO_conf16		Slanted	Aldehyde O & C	-2.405
NiO_conf17		Slanted	Aldehyde O	-1.601
NiO_conf18		Slanted	Aldehyde O & C	-2.404
NiO_conf19		Slanted	Aldehyde O & C Furanic O	-2.449

The systems in which the furfural molecule is adsorbed via aldehydic O and C and the O-atom in the furanic ring was seen to be most stable.

Table S3. The orientation of furfural before and after relaxation followed by the nature of interaction after relaxation and the adsorption energies in different models of furfural on TiO_2(111) surface.

System	orientation		Bonded through	Ead
	Initial	Final		
TiO_2_conf1	parallel	slightly slanted	None	-0.963
TiO_2_conf2		slightly slanted	None	-0.796
TiO_2_conf3		slanted	C of CHO	-0.484
TiO_2_conf4		slanted	C of furanic ring to O	-4.113
TiO_2_conf5			C and O of CHO to O	-1.633
TiO_2_conf6	perpendicular	perpendicular	O of CHO to Ti	-1.138
TiO_2_conf7			O of CHO to Ti	-1.061
TiO_2_conf8			O of CHO to Ti	-1.187
TiO_2_conf9			O of CHO to Ti	-1.056
TiO_2_conf10			O of CHO to Ti	-1.126